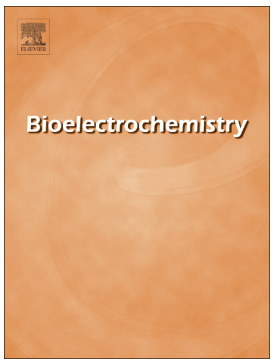

Peptide nucleic acid as a selective recognition element for electrochemical determination of Hg2+

Agnieszka Bala, Łukasz Górski

PII: S1567-5394(17)30400-0
DOI: doi:10.1016/j.bioelechem.2017.09.008
Reference: BIOJEC 7053

To appear in: *Bioelectrochemistry*

Received date: 4 August 2017
Revised date: 15 September 2017
Accepted date: 15 September 2017

Please cite this article as: Agnieszka Bala, Łukasz Górski , Peptide nucleic acid as a selective recognition element for electrochemical determination of Hg2+. The address for the corresponding author was captured as affiliation for all authors. Please check if appropriate. Biojec(2017), doi:10.1016/j.bioelechem.2017.09.008

Peptide nucleic acid as a selective recognition element for electrochemical determination of Hg^{2+}

Agnieszka Bala, Łukasz Górski*

[1] Institute of Biotechnology, Department of Microbioanalytics, Faculty of Chemistry, Warsaw University of Technology, Noakowskiego 3, 00-664 Warsaw, Poland

*Corresponding author. Tel.: +48 222 347573, Fax: +48 226 282741. E-mail address: lukegor@ch.pw.edu.pl (Ł. Górski)

Abstract

A novel electrochemical PNA-based biosensor for the determination of Hg^{2+} is described. The receptor layer, containing single strands of polythymine PNA (peptide nucleic acid), was formed at the surface of gold electrode. Due to the presence of thymine bases and peptide bonds, an interaction between Hg^{2+} ion and receptor layer occurs. The influence of chain modification – PNA *vs.* DNA – and type of redox marker – anionic AQMS-Na (sodium salt of anthraquinone-2-sulfonic acid) and $Fe^{II/III}$ (potassium ferri/ferrocyanide) or cationic MB (methylene blue) and RuHex (hexaammineruthenium(III) chloride) – were studied. Proposed PNA-based biosensor with anionic AQMS-Na as a redox marker demonstrated significantly better analytical parameters, as compared to results obtained for other tested redox markers (for measurements at pH 6.0). The linear response towards Hg^{2+} was in the range from 5 to 500 nmol·L^{-1} with the detection limit of 4.5 nmol·L^{-1}. The developed sensor distinguishes itself with high selectivity towards Hg^{2+}, even for solutions containing several interfering cations. Interactions between Hg^{2+} and PNA receptor layer were studied using square wave voltammetry (SWV) and electrochemical impedance spectroscopy (EIS).

Keywords: PNA sensor; thymine bases; voltammetry; mercury ion; redox marker

1. Introduction

The monitoring of highly toxic metals such as mercury (as a water-soluble Hg^{2+} ion as well as various complexes and organomercury compounds) is of paramount importance. Human exposure to mercury can have negative effects on health, including kidney failure [1] or brain damage [2]. Currently, colorimetric assays [3], inductively coupled plasma mass spectroscopy [4] and fluorescence spectroscopy [5] are methods commonly used for Hg^{2+} determination. However, due to high cost and complicated instrumentation, cheaper and less sophisticated methods are needed. Electrochemical biosensors seem to be excellent approach for determination of Hg^{2+} due to high sensitivity and selectivity, low cost and simplicity [6-8]. As recognition elements, various molecules of biological origin such as enzymes, nucleic acids, antibodies or whole cells can be used [9]. The most common application of DNA-based biosensors is detection of specific nucleic acid sequences, important e.g. in the field of diagnosis of genetic diseases [10]. However, owing to the structure of DNA, interactions with other molecules, including metal ions, are possible [11]. So far, great deal of work has been done on the development of biosensors dedicated to metal ions determination, employing electrochemical properties of DNA [12, 13]. Unfortunately, due to limited stability and possibility of non-specific interactions of interfering species with receptor layer, utilization of DNA-based biosensor can be limited.

Among the wide range of electrochemical biosensors dedicated to the determination of mercuric ion, the most popular are those based on thymine–Hg^{2+}–thymine (T–Hg^{2+}–T) interaction. It was confirmed that binding of Hg^{2+} by two thymine bases is specific and strong, as T–Hg^{2+}–T bond is more stable, as compared to Watson-Crick adenine–thymine interaction [14-20]. Interactions between Hg^{2+} and different nitrogen bases, including U–

Hg^{2+}–U [21], T–Hg^{2+}–C and A–Hg^{2+}–T [22, 23], were studied using IR, Raman and NMR spectroscopy, however, none of these complexes was used for sensor development.

One of the latest reports dealing with the determination of Hg^{2+} using T–Hg^{2+}–T interaction was based on electrochemical label-free aptasensor [24]. In the absence of Hg^{2+}, hybridization event occurs between single stranded DNA (ssDNA), immobilized on gold surface, and complementary strand of DNA (cDNA). In turn, addition of even zeptomolar amount of Hg^{2+} results in dsDNA denaturation due to interaction between cDNA and Hg^{2+}, resulting in formation of T–Hg^{2+}–T complex.

Recently, several studies were published on the detection of Hg^{2+} based on interactions between this analyte and nitrogen (N), oxygen (O) or sulfur (S) atoms present in the structure of peptides [25-29]. The strength of this interaction depends on the pH of the environment, presence of the aromatic rings, kind of donor atoms and hardness/softness of coordinated metal. Moreover, it was shown that the length of polypeptides influence on the strength of metal ions binding by receptor layer containing these molecules.

What is worth mentioning, peptide nucleic acids (PNAs) are also able to interact with metal ions [30, 31]. However, most of developed PNA-based biosensors are dedicated to the determination of complementary DNA sequences [32-36]. Nevertheless, due to the presence of peptide chain, similarity between PNA and peptides is high, what makes this molecule excellent candidate for development of receptor layers for metal ions determination. One of the examples is work presented by Gao et al. [30]. This study is based on electrochemical impedance investigations of single or double stranded PNA films in the presence of different metal ions such as Zn^{2+}, Co^{2+}, Ni^{2+} and Mg^{2+}. It was shown that only for Mg^{2+}, no changes in impedance properties of PNA films were observed. Similar approach was also utilized by Li et al. [31]. Authors performed EIS (electrochemical impedance spectroscopy) measurements of

mixed PNA-DNA film after addition of Mg^{2+}, Zn^{2+}, Co^{2+} and Ni^{2+}. It was concluded that beyond of electrostatic interaction between PNA-DNA film and metal ions, the strongest binding was observed in case of Ni^{2+}. For other tested cations, recorded EIS response was negligible.

Based on above-mentioned results, our group decided to use PNA as receptor layer immobilized on the surface of gold electrodes [37]. PNA was of random sequence, thus it was assumed that the interaction between Hg^{2+} and PNA is based on binding between this metal cation and carbonyl oxygen and/or amide nitrogen from peptide PNA backbone. These assumptions have been confirmed by spectrophotometric studies. Recorded UV-VIS absorption spectra clearly showed that increase of Hg^{2+} concentration in PNA solution resulted in a significant increase of the absorption band centered at 210 nm. These results demonstrated the formation of complexes between Hg^{2+} and peptide moieties from PNA backbone, what is in good agreement with reported Hg^{2+}-peptide interactions [25]. In addition, working parameters of proposed PNA-based biosensor were remarkably good, with linear response in the range of 0.05 to 10 $\mu mol \cdot L^{-1}$ and lower detection limit of 3.33 $nmol \cdot L^{-1}$ which is lower than the toxic level for Hg^{2+} defined by the EPA. In addition, selectivity of proposed biosensor was good.

Encouraged by previous results, we decided to continue the development of PNA-based biosensors for Hg^{2+} determination. Herein, we present further studies based on the use of single strands of PNA containing only thymine bases (previously, random PNA sequence was used, thus interactions between PNA receptor layer and Hg^{2+} were based on complexation of Hg^{2+} by peptide moieties from PNA backbone). Herein, the enhancement of binding of Hg^{2+} by PNA receptor layer was observed due to formation of T–Hg^{2+}–T complex as well as interactions of Hg^{2+} with PNA backbone. Similar to previous work, self-assembled

monolayer of PNA was obtained by immobilization of single-stranded PNA modified with thiol group. To generate current signal, anionic redox marker – sodium salt of anthraquinone-2-sulfonic acid (AQMS-Na) – was used. The analytical signal was measured as the changes of registered current value – derived from AQMS-Na – before and after incubation in Hg^{2+} solution. In order to study interactions between Hg^{2+} and PNA receptor layer, square wave voltammetry (SWV) and electrochemical impedance spectroscopy (EIS) were used.

2. Materials and methods

2.1. Apparatus

Voltammetric studies were performed with CHI 660A and CHI 1040A electrochemical workstations (CH Instruments, USA). Electrochemical impedance spectroscopy (EIS) measurements were performed with a CHI 660A electrochemical workstation. The measurements were carried out with a conventional three-electrode system consisting of a gold disk electrode (CH Instruments, USA), a gold wire auxiliary electrode and an Ag/AgCl/1.0 $mol \cdot L^{-1}$ KCl reference electrode. All potentials are reported versus Ag/AgCl reference electrode at room temperature.

Square wave voltammetry (SWV) measurements were performed at a pulse amplitude of 25 mV, increment of 4 mV, and a frequency of 15 Hz.

EIS was carried out at a dc potential of -500 mV and the ac amplitude was 5 mV. Frequency was in the range from 0.1 Hz to 100 kHz. EIS results were analyzed based on the equivalent circuit consisting of a resistor connected in series to a capacitor.

2.2. Reagents

Tris, methylene blue (MB), sodium salt of anthraquinone-2-sulfonic acid (AQMS-Na), hexaammineruthenium(III) chloride (RuHex), potassium ferri/ferrocyanide ($K_4Fe(CN)_6/K_3Fe(CN)_6$), 6-mercapto-1-hexanol (MCH), mercury(II) chloride, copper(II) nitrate, magnesium nitrate, potassium nitrate, lead nitrate, cobalt nitrate, barium chloride, tin nitrate, cadmium nitrate, uranyl acetate, calcium nitrate, NaOH and KH_2PO_4 were purchased from Aldrich Chemicals. H_2SO_4, HNO_3, ethanol and H_2O_2 were purchased from POCh, Poland. All reagents were used without further purification. All solutions were prepared with Milli-Q water. Milli-Q water and all aqueous solutions were sterilized using an autoclave. Peptide nucleic acids were purchased from Panagene (Daejeon, Korea). The PNA probes used in this study were thiolated at their N-terminal positions. Deoxyoligonucleotides were purchased from Genomed Sp. z o.o., Poland.

The base sequences used in this work were as follows (all used probes were thiolated DNA or PNA oligonucleotides):

PNA: (N-term) HS-TTTTTTTTTT (C-term)

DNA: 5'-HS-TTTTTTTTTT-3'

Oligonucleotide stock solutions were prepared with 10 mmol·L^{-1} Tris - HCl, (pH 7.5) and stored in a − 20 °C freezer before use.

2.3. Solutions

The following solutions were prepared: piranha solution (H_2O_2/H_2SO_4; 1:3), immobilization solution (1 mol·L^{-1} KH_2PO_4, pH 4.5), 100 µmol·L^{-1} or 4 µmol·L^{-1} MCH in 1 mol·L^{-1} KH_2PO_4 (pH 4.5), Tris solution (10 mmol·L^{-1}, pH 6.0), $HgCl_2$ solution in 10 mmol·L^{-1} Tris solution, $Cu(NO_3)_2/Mg(NO_3)_2/KNO_3/Pb(NO_3)_2/Co(NO_3)_2/BaCl_2/Sn(NO_3)_2/Cd(NO_3)_2/Ca(NO_3)_2/UO_2(CH_3COO)_2$ solutions in 10 mmol·L^{-1} Tris solution containing 1 mmol·L^{-1} AQMS-

Na/1 mmol·L^{-1} $K_3[Fe(CN)_6]/K_4[Fe(CN)_6]$ (1:1) in 0.1 mol·L^{-1} KCl solution/10 µmol·L^{-1} RuHex/10 µmol·L^{-1} MB.

Voltammetric measurements were carried out in 10 mmol·L^{-1} Tris containing 1 mmol·L^{-1} AQMS-Na/1 mmol·L^{-1} $K_3[Fe(CN)_6]/K_4[Fe(CN)_6]$ (1:1) in 0.1 mol·L^{-1} KCl solution/10 µmol·L^{-1} RuHex/10 µmol·L^{-1} MB. The "mix" solution contained all cations mentioned above (the concentration of each cation was 10 µmol·L^{-1}). The EIS measurements were performed in 10 mmol·L^{-1} Tris solution containing 1 mmol·L^{-1} AQMS-Na. The pH was adjusted with 1 mol·L^{-1} NaOH or HCl aqueous solutions.

2.4. Methods

Before any electrochemical experiments, gold electrodes were polished with alumina powder of grain sizes from 1 to 0.05 µm (CH Instruments, USA). Then, electrodes were washed with demineralized water and sonicated for 2 minutes at 40 °C in water/ethanol mixture (volume ratio: 1/1). Next, the piranha solution was dropped on the working gold disk electrode and incubated for 1 minutes. After removing the solution, the electrode was washed with demineralized water. The last step of electrode cleaning was its voltammetric cycling in 500 mmol·L^{-1} H_2SO_4 solution, until the CV characteristic for a clean gold was obtained.

DNA or PNA recognition monolayer was prepared as follows: after the electrode cleaning, 25 µL of 4 µmol·L^{-1} solution of thiolated ssDNA or ssPNA in 1 mol·L^{-1} KH_2PO_4 (pH 4.5) was dropped on the gold disc electrode. The ssDNA or ssPNA immobilization was carried out for 120 minutes. Then electrode was incubated in 4 µmol·L^{-1} solution of MCH for 30 minutes. Finally, the solution was removed and the electrode was washed with immobilization solution and the electrochemical measurements were conducted.

The sensor response was defined with the use of the following equation:

$$\Delta = (I-I_0)/I_0$$

where I_0 refers to AQMS-Na oxidation current before and I to the AQMS-Na oxidation current after the 60 minutes incubation in the sample solution containing Hg^{2+} ions.

3. Results and discussion

3.1. Selection of redox marker

In this work, biosensors with peptide nucleic acid (PNA) receptor layers for determination of mercury cation (Hg^{2+}) are described. Single strands of PNA contain only thymine bases, while thiol modification allows for formation of self-assembled monolayers of PNA strands at the surface of gold electrode. 6-mercapto-1-hexanol (MCH) was used as a blocking agent for PNA receptor layer. This allowed to remove weakly adsorbed single strands of PNA. In addition, possibility of non-specific interactions of redox marker and analyte with electrode surface was reduced.

In order to choose the most appropriate redox marker, four compounds were tested during preliminary studies: sodium salt of anthraquinone-2-sulfonic acid (AQMS-Na) and potassium ferri/ferrocyanide ($Fe^{II/III}$) as anionic redox markers, as well as methylene blue (MB) and hexaammineruthenium (III) chloride (RuHex) as cationic redox markers. Charge of redox marker is an important factor influencing its interactions with receptor molecules. Based on literature reports [38-41] and our previous work [42-44] it can be concluded that in the absence of target ion (Hg^{2+}), access of redox marker to the electrode surface is relatively easy. Binding of positively charged Hg^{2+} with PNA receptor layer causes a decrease of the amount of redox marker in the vicinity of electrode surface (for positive charged markers) or its increase (for negative charged markers). The concentration of the redox marker is measured electrochemically and the changes in registered current value can be correlated with Hg^{2+} concentration.

As it can be seen in Figure 1, the highest current changes were registered for negatively charged AQMS-Na (Δ=1.64±0.03). Surprisingly, for anionic $Fe^{II/III}$, a decrease of current value after incubation in Hg^{2+} solution was observed with total current change of –

0.51±0.03. For cationic MB and RuHex redox markers, registered current changes were as follows: Δ_{MB}= –0.15±0.05 and Δ_{RuHex}= –0.24±0.03. Based on these results, anionic AQMS-Na and $Fe^{II/III}$ markers were chosen for further experiments.

3.2. Electrochemical behavior of the modified electrode

In the first step, influence of surface modification with single strands of PNA was tested. As it can be seen in Figure 2, peak current derived from AQMS-Na (Figure 2A) and $Fe^{II/III}$ (Figure 2B) for unmodified electrode is pronounced (curve I). Next, after immobilization of PNA, for AQMS-Na (Figure 2A), peak derived from redox marker is splitted into two separate peaks. This behavior can be explained by the presence of two forms of AQMS-Na [37, 45, 46]. One of them (Ep –0.670 V) origins from free AQMS-Na, while the other peak, recorded at Ep of –0.300 V, is derived from AQMS-Na interacting with PNA receptor layer (curve II in Figure 2A). In turn, incubation in solution containing Hg^{2+} causes significant increase of current value for AQMS-Na that interacts with PNA receptor layer (curve III). In addition, shift of current peak toward more negative potential is observed but this change is negligible. Based on these results, it can be assumed that Hg^{2+} binds to single strands of PNA, present within the receptor layer (see Scheme 1).

Similar behavior – an increase of current value after incubation in Hg^{2+} solution – was also expected in the case of $Fe^{II/III}$ (due to anionic character of $Fe^{II/III}$). After modification with single stranded PNA (curve II), registered current value diminished (as compared with current value for unmodified electrode – curve I) what is connected with steric hindrance caused by receptor layer and limited access of redox marker to the electrode surface. Surprisingly, after incubation in Hg^{2+} solution, a decrease of current value derived from $Fe^{II/III}$ was observed (curve III). Possibly, this behavior can be connected with the different

structures of AQMS-Na and $Fe^{II/III}$. These differences can influence the mobility of redox marker in the vicinity of receptor layer after incubation in solution containing Hg^{2+}. As it was mentioned, structures of utilized molecules (AQMS-Na and $Fe^{II/III}$) are completely different: AQMS-Na is organic flat structure, while $Fe^{II/III}$ is inorganic molecule with coordination number 6 what makes it branched molecule. For AQMS-Na, increase of current value is observed due to electrostatic interactions (anionic AQMS-Na – cationic Hg^{2+}) and possibility of slipping flat molecules of AQMS-Na between PNA strands. In turn, in case of $Fe^{II/III}$, after complexation of Hg^{2+} by PNA receptor layer, interaction of redox marker with electrode surface is limited due to structure of $Fe^{II/III}$. After binding of Hg^{2+} by receptor layer, densely packed monolayer is obtained due to the formation of T–Hg^{2+}–T complexes. Therefore, access to the electrode surface and mobility of branched $Fe^{II/III}$ between PNA strands is significantly reduced. As a result, lower amount of $Fe^{II/III}$ reaches electrode surface (comparing with amount before incubation in Hg^{2+}) what causes decrease of current signal derived from $Fe^{II/III}$ marker.

For both redox makers, concentration of Hg^{2+} can be correlated with measured changes of AQMS-Na or $Fe^{II/III}$ current. Sensor response is defined as $\Delta=(I-I_0)/I_0$, thus it possible to reduce influence of changes of the electrochemical area of an electrode and imperfections of receptor layer.

In both cases, current changes were registered (before and after 60 minutes incubation in 10 $\mu mol \cdot L^{-1}$ Hg^{2+} solution) and obtained data were as follows: 1.64±0.03 and -0.51±0.03 for AQMS-Na and $Fe^{II/III}$, respectively. As it can be seen, for AQMS-Na significantly higher current changes were registered. In addition, initial measurements allowing for determination of calibration curve were performed. For AQMS-Na, linear response towards Hg^{2+} concentration was observed in the range from 5 to 500 $nmol \cdot L^{-1}$. For $Fe^{II/III}$ linear range

was observed at higher concentrations of Hg^{2+} (0.5 to 10 µmol·L^{-1}). Based on these preliminary studies, AQMS-Na was chosen for further experiments.

3.3. Optimization of working parameters

Incubation time

Time of analysis is one of the most important parameters, determining the usefulness of proposed biosensor. Current change for PNA-based biosensor with AQMS-Na as a redox marker was recorded for several incubation times. Obtained results were as follows: Δ_{10} = 0.44±0.03; Δ_{30} = 0.48±0.03; Δ_{45} = 0.75±0.04; Δ_{60} = 1.64±0.03 and Δ_{90} = 0.82±0.04. As it can be seen, the highest current change was registered for 60 minutes incubation time, while elongation of this parameter resulted in a decrease of current change (probably due to the saturation of receptor layer).

PNA vs DNA

The influence of backbone modification on sensor response was also tested (for both redox markers). As it can be seen in Figure 3A, both for AQMS-Na and $Fe^{II/III}$, significantly better results were observed in case of PNA modification ($\Delta_{AQMS\text{-}Na}$ = 1.64±0.03 and $\Delta_{Fe}^{II/III}$ = -0.51±0.03). For electrodes modified with DNA (with the same base sequence), registered current changes were twice (0.84±0.04 for AQMS-Na) and four times (-0.14±0.02 for $Fe^{II/III}$) lower as compared to current changes registered for PNA-modified electrode. These data clearly indicate that the use of PNA in the receptor layer is more beneficial for Hg^{2+} determination than modification of electrode surface with DNA strands.

Peak current vs scan rate

CV measurements in Tris solution containing AQMS-Na were performed to observe the dependence between peak current and scan rate (from 5 to 500 $mV \cdot s^{-1}$). In Figure 3B, a linear dependence between peak current and the square root of scan rate can be seen with the following equations: I_{pc} [µA] = -15.2v $[(V \cdot s^{-1})^{1/2}]$ – 2.1 (R^2 = 0.99); I_{pa} [µA] = 17.1v $[(V \cdot s^{-1})^{1/2}]$ + 0.4 (R^2 = 0.98) before incubation in Hg^{2+} and I_{pc} [µA] = -20.3v $[(V \cdot s^{-1})^{1/2}]$ – 2.4 (R^2 = 0.99); I_{pa} [µA] = 24.8v $[(V \cdot s^{-1})^{1/2}]$ – 1.0 (R^2 = 1.00) after incubation in Hg^{2+}. These results revealed that the redox reaction of AQMS-Na is controlled by diffusion before and after incubation in Hg^{2+} solution. The rate of AQMS-Na diffusion is determined by the charge of the receptor layer which is influenced by the amount of Hg^{2+} interacting with PNA strands, immobilized on the gold electrode.

3.4. Electrochemical impedance spectroscopy

Electrochemical impedance spectroscopy (EIS) was utilized to investigate the impedance change at the electrode surface after consecutive steps of surface modification. The measured impedance data can be matched by experimental model – Randles circuit – that contains four equivalent circuit elements: solution resistance (R_s), double layer capacitance (C_{dl}), electron transfer resistance (R_{ct}) and Warburg impedance (Z_w) (see Inset of Figure 4).

All measurements were performed in Tris solution containing AQMS-Na as a redox marker. As it can be observed in Figure 4, for unmodified gold electrode (curve I), small semicircle, with R_{ct} of 0.7 kΩ, was recorded. Significant increase of R_{ct} value (258.2 kΩ) is observed after modification of gold surface with single strands of PNA (curve II) what can be connected with the steric hindrance caused by receptor layer. After incubation of PNA-modified electrode in solution containing Hg^{2+}, R_{ct} value decreased more than twice to 102.2

kΩ (curve III) what suggests that charge-transfer process is faster (compared with data obtained for PNA-based biosensor before incubation in Hg^{2+}). Probably, incubation in Hg^{2+} solution causes an increase of the receptor layer charge due to the complexing of Hg^{2+} by PNA, and anionic AQMS-Na is attracted by positively charged receptor layer.

3.5. Quantitative determination of Hg^{2+}

In the next step, in order to assess the usefulness of the proposed PNA-modified electrode, the measured changes in AQMS-Na current were plotted against the concentration of Hg^{2+}. These results are presented in Figure 5. It can be observed that an increase of Hg^{2+} concentration causes increase of measured AQMS-Na current change. The dependence between analytical signal and logarithmic value of Hg^{2+} concentration, shown in the inset to Figure 5, is related to the logarithmic shape of adsorption isotherm. The linear range of the calibration curve can be observed from 5 to 500 nmol·L^{-1} with the detection limit of 4.5 nmol·L^{-1}, calculated as 3δ, where δ is standard deviation registered for blank sample. For higher concentrations of Hg^{2+}, calibration curve flattening was observed. Determined value of detection limit is lower than the toxic level for Hg^{2+} defined by the EPA.

3.6. Detection of Hg^{2+} in environmental water samples

Practical application of developed biosensors is very important e.g. for determination of heavy metal ions in real water samples. Therefore, the utility of proposed PNA-based biosensor for Hg^{2+} determination was checked by performing measurements for tap water spiked with Hg^{2+}. The concentration of AQMS-Na in these solutions was 1 mmol·L^{-1}, while the pH value of solution was 6.0 (10 mmol·L^{-1} Tris). In prepared solution, final concentration of Hg^{2+} was as follows: 25 nmol·L^{-1} (sample 1) and 500 mmol·L^{-1} (sample 2). Recorded current

changes were as follows: 0.386±0.024 for sample 1 and 0.927±0.031 for sample 2 what corresponds to Hg^{2+} concentration of 24.15 nmol·L^{-1} and 519.42 nmol·L^{-1}, respectively. The recovery of Hg^{2+} was between 96.62% for sample 1 and 103.88% for sample 2 which indicate that proposed biosensor can be used in monitoring of Hg^{2+} in environmental samples.

3.7. Selectivity

The last step of performed measurements was the assessment of the selectivity of proposed biosensor. Selectivity was investigated against some common metal ions (see Figure 6A). This parameter was also tested for solution containing all of the examined cations with Hg^{2+} ("mix"). Concentration of each tested cation was 10 µmol·L^{-1} while incubation time before and after incubation in metal cation solution was 10 minutes and 60 minutes, respectively. As it can be seen in Figure 6A, the highest signal response was recorded for Hg^{2+} (Δ = 1.64±0.03). Only for K^{+}, Pb^{2+} and Cd^{2+} an increase of current signal was recorded but these values were more than three times lover than for Hg^{2+} (0.43±0.07 for K^{+}, 0.27±0.02 for Pb^{2+} and 0.13±0.01 for Cd^{2+}). On the contrary, for the rest of examined metal cations, decrease of current was registered. Also for “mix” solution significant response was observed – similar to value obtained for solution containing only Hg^{2+}. This can be explained by strong interaction between Hg^{2+} and receptor layer. The presence of Hg^{2+} blocks the access of interfering ions to the receptor layer and, as a result, additivity of sensor response for different ions is not observed in "mix" sample. These results clearly indicate that even in the presence of interfering ions, proposed sensor is highly selective toward Hg^{2+}.

The selectivity of proposed biosensor was also checked for lower concentrations of Hg^{2+} and K^{+} (due to the most significant interfering effect amongst all examined metal cations). As it can be seen in Figure 6B, recorded current change for solution containing only

Hg^{2+} in concentration of 50 nmol·L^{-1} was 0.50±0.02. Measurements were also performed for Hg^{2+} solution (50 nmol·L^{-1}) containing K^+ at concentrations of 50 nmol·L^{-1} and 1 µmol·L^{-1}. In these cases, registered current changes were 0.48±0.02 and 0.48±0.03, respectively. Moreover, for solution containing only 1 µmol·L^{-1} K^+, insignificant biosensor response was recorded (0.16±0.02). Presented results clearly indicate that even for lower concentration of Hg^{2+}, selectivity of PNA-biosensor is high (addition of K^+ does not influence on biosensor response).

This behavior of PNA-based biosensor is based on thymine – Hg^{2+} – thymine and Hg^{2+} – peptide moieties interactions what was proven in this work and earlier literature reports. Presented data confirm the selectivity of PNA/MCH-based biosensor towards Hg^{2+}.

4. Conclusions

Herein, a polythymine PNA-based biosensor was proposed for the determination of Hg^{2+} in water samples. Recognition of Hg^{2+} by receptor layer is based on interaction between Hg^{2+} and thymine bases present in the backbone of utilized PNA sequence. Moreover, the strength of this interaction is enhanced by coordination of Hg^{2+} by peptide moieties from PNA chain. In order to generate current signal, external redox marker – anionic AQMS-Na – was used. It was shown that an increase of Hg^{2+} concentration results in higher current changes derived from AQMS-Na. The linear response for proposed PNA-biosensor was registered for Hg^{2+} in the concentration range from 5 to 500 $nmol \cdot L^{-1}$ with the detection limit of 4.5 $nmol \cdot L^{-1}$. Furthermore, the selectivity of proposed biosensor towards Hg^{2+} is good what demonstrates the feasibility of PNA-based biosensor for monitoring Hg^{2+} concentration in real water samples.

Acknowledgements

This work was financially supported by Warsaw University of Technology.

References:

[1] E. Saball, M. Salvarrey, E. Serra, G. Picó, M.M. Elías, Potential mechanism of fibronectin deposits in acute renal failure induced by mercuric chloride, Mol. Cell. Biochem. 226 (2001) 67–75.
[2] J. Albrecht, E. Matyja, Glutamate: A potential mediator of inorganic mercury neurotoxicity, Metab. Brain Dis. 11 (1996) 175–184.
[3] C. Li, P. Dai, X. Rao, L. Shao, G. Cheng, P. He, Y. Fang, An ultra-sensitive colorimetric Hg^{2+}-sensing assay based on DNAzyme-modified Au NP aggregation, MNPs and an endonuclease, Talanta 132 (2015) 463–468.
[4] K.-j. Chen, I.-h. Hsu, Y.-c. Sun, Determination of methylmercury and inorganic mercury by coupling short-column ion chromatographic separation, on-line photocatalyst-assisted vapor generation, and inductively coupled plasma mass spectrometry, J. Chromatogr. A 1216 (2009) 8933–8938.
[5] T.-M. Geng, X. Wang, H. Jiang, W. Song, R.-F. Ni, J. Chen, Y. Wang, Fluorescent Polyamide-Based Rhodamine Hydrazide Moieties with Oxethyl as Spacer for Detection of Cr^{3+}, Fe^{3+}, and Hg^{2+} Ions in Water, J. Fluoresc. 26 (2016) 977–985.
[6] C. Lu, H. Yang, C. Zhu, X. Chen, G. Chen, A graphene platform for sensing biomolecules, Angew. Chem. Int. Edit. 28 (2009) 4785–4787.
[7] B. Song, D. Li, W. Qi, M. Elstner, C. Fan, H. Fan, Graphene on Au(111): A highly conductive material with excellent adsorption properties for high-resolution bio/nanodetection and identification, ChemPhysChem 11 (2010) 585–589.
[8] D. Tang, J. Tang, Q. Li, B. Su, G. Chen, Ultrasensitive aptamer-based multiplexed electrochemical detection by coupling distinguishable signal tags with catalytic recycling of DNase I, Anal. Chem. 83 (2011) 7255–7259.
[9] J.P. Chambers, B.P. Arulanandam, L.L. Matta, A. Weis, J.J. Valdes, Biosensor recognition elements, Curr. Issues Mol. Biol. 10 (2008) 1-12.
[10] A. Sassolas, B.D. Leca-Bouvier, L.J. Blum, DNA biosensors and microarrays, Chem. Rev. 108 (2008) 109–139.
[11] J. Liu, Z. Cao, Y. Lu, Functional nucleic acid sensors, Chem. Rev. 109 (2009) 1948–1998.
[12] E. Palecek, M. Bartosik, Electrochemistry of nucleic acids, Chem. Rev. 112 (2012) 3427–3481.
[13] W. Zhou, R. Saran, J. Liu, Metal Sensing by DNA, Chem. Rev. 117 (2017) 8272–8325.
[14] M. Lu, R. Xiao, X. Zhang,J. Niu,X. Zhang,Y. Wang, Novel electrochemical sensing platform for quantitative monitoring of Hg(II) on DNA-assembled graphene oxide with target recycling, Biosens. Bioelectron. 85 (2016) 267–271.
[15] J. Chen, J. Tang, J. Zhou, L. Zhang, G. Chen, D. Tang, Target-induced formation of gold amalgamation on DNA-based sensing platform for electrochemical monitoring of mercury ion coupling with cycling signal amplification strategy, Anal. Chim. Acta 810 (2014) 10–16.
[16] M. Xu, Z. Gao, Q. Wei, G. Chen, D. Tang, Label-free hairpin DNA-scaffolded silver nanoclusters for fluorescent detection of Hg^{2+} using exonuclease III-assisted target recycling amplification, Biosens. Bioelectron. 79 (2016) 411–415.
[17] F. Long, A. Zhu, H. Shi, H. Wang, J. Liu, Rapid on-site/in-situ detection of heavy metal ions in environmental water using a structure-switching DNA optical biosensor, Sci. Rep.-UK 3 (2013) art no. 2308.

[18] L. Shi, Z. Chu, Y. Liu, W. Jin, X. Chen, An ultrasensitive electrochemical sensing platform for Hg^{2+} based on a density controllable metal-organic hybrid microarray, Biosens. Bioelectron. 54 (2014) 165–170.
[19] F. Maâtouk, M. Maâtouk, K. Bekir, H. Barhoumi, A. Maaref, H.B. Mansour, An electrochemical DNA biosensor for trace amounts of mercury ion quantification, J. Water Health 14 (2016) 808–815.
[20] Y. Zhu, Y. Cai, Y. Zhu, L. Zheng, J. Ding, Y. Quan, L. Wang, B. Qi, Highly sensitive colorimetric sensor for Hg^{2+} detection based on cationic polymer/DNA interaction, Biosens. Bioelectron. 69 (2015) 174–178.
[21] S. Johannsen, S. Paulus, N. Dupre, J. Muller, R.K. Sigel, Using in vitro transcription to construct scaffolds for one-dimensional arrays of mercuric ions, J. Inorg. Biochem. 102 (2008) 1141−1151.
[22] A. Ono, H. Torigoe, Y. Tanaka, I. Okamoto, Binding of metal ions by pyrimidine base pairs in DNA duplexes, Chem. Soc. Rev. 40 (2011) 5855−5866.
[23] Y. Tanaka, J. Kondo, V. Sychrovsky, J. Sebera, T. Dairaku, H. Saneyoshi, H. Urata, H. Torigoe, A. Ono, Structures, physicochemical properties, and applications of T-Hg^{II}-T, C-Ag^{I}-C, and other metallo-base-pairs, Chem. Commun. 51 (2015) 17343−17360.
[24] S. Amiri, A. Navaee, A. Salimi, R. Ahmadi, Zeptomolar detection of Hg^{2+} based on label-free electrochemical aptasensor: One step closer to the dream of single atom detection, Electrochem. Commun. 78 (2017) 21–25.
[25] S. Pires, J. Habjanič, M. Sezer, C.M. Soares, L. Hemmingsen, O. Iranzo, Design of a peptidic turn with high affinity for Hg^{II}, Inorg. Chem. 51 (2012) 11339–11348.
[26] A. Fragoso, T. Carvalho, P. Rousselot-Pailley, M.M. Correia Dos Santos, R. Delgado, O. Iranzo, Effect of the Peptidic Scaffold in Copper(II) Coordination and the Redox Properties of Short Histidine-Containing Peptides, Chem. Eur. J. 21 (2015) 13100–13111.
[27] C. Lebrun, M. Starck, V. Gathu, Y. Chenavier, P. Delangle, Engineering Short Peptide Sequences for Uranyl Binding, Chem. Eur. J. 20 (2014) 16566–16573.
[28] E. Chow, J.J. Goading, Peptide modified electrodes as electrochemical metal ion sensors, Electroanal. 18 (2006) 1437–1448.
[29] J.J. Gooding, D.B. Hibbert, W. Yang, Electrochemical metal ion sensors. Exploiting amino acids and peptides as recognition elements, Sensors 1 (2001) 75–90.
[30] L. Gao, C. Li, X. Li, H.-B. Kraatz, Electrochemical impedance study of the interaction of metal ions with unlabeled PNA, Chem. Commun. 46 (2010) 6344-6346.
[31] C. Li, X. Li, X. Liu, H.-B. Kraatz, Exploiting the interaction of metal ions and peptide nucleic acids - DNA duplexes for the detection of a single nucleotide mismatch by electrochemical impedance spectroscopy, Anal. Chem. 82 (2010) 1166-1169.
[32] J. Wang, E. Palecek, P.E. Nielsen, G. Rivas, X. Cai, H. Shiraishi, N. Dontha, D. Luo, P.A.M. Farias, Peptide nucleic acid probes for sequence-specific DNA biosensors, J. Am. Chem. Soc. 118 (1996) 7667–7670.
[33] D. Ozkan, A. Erdem, P. Kara, K. Kerman, J.J. Gooding, P.E. Nielsen, M. Ozsoz, Electrochemical detection of hybridization using peptide nucleic acids and methylene blue on self-assembled alkanethiol monolayer modified gold electrodes, Electrochem. Commun. 4 (2002) 796–802.
[34] H. Gaiji, P. Jolly, S. Ustuner, S. Goggins, M. Abderrabba, C.G. Frost, P. Estrela, A Peptide Nucleic Acid (PNA)-DNA Ferrocenyl Intercalator for Electrochemical Sensing, Electroanal. 28 (2016) 1–7.

[35] D. Ozkan, P. Kara, K. Kerman, B. Meric, A. Erdem, F. Jelen, P.E. Nielsen, M. Ozsoz, DNA and PNA sensing on mercury and carbon electrodes by using methylene blue as an electrochemical label, Bioelectrochem. 58 (2002) 119–126.
[36] P. Kara, K. Kerman, D. Ozkan, B. Meric, A. Erdem, P.E. Nielsen, M. Ozsoz, Label-free and label based electrochemical detection of hybridization by using methylene blue and peptide nucleic acid probes at chitosan modified carbon paste electrodes, Electroanal. 14 (2002) 1685–1690.
[37] A. Bala, K. Zalewski, Ł. Górski, Electrochemical determination of Hg^{2+} using electrodes modified with peptide nucleic acid, J. Electrochem. Soc. 163 (2016) B667–B672.
[38] D. L. Peng, H.F. Ji, X.D. Dong, J.F. Tian, M.H. Wang, L.H. He, Z.Z. Zhang, S.M. Fang, Highly Sensitive Electrochemical Bioassay for Hg(II) Detection Based on Plasma-Polymerized Propargylamine and Three-Dimensional Reduced Graphene Oxide Nanocomposite, Plasma Chem. Plasma Process. 36 (2016) 1051–1065.
[39] M. Wang, S. Zhang, Z. Ye, D. Peng, L. He, F. Yan, Y. Yang, H. Zhang, Z. Zhang, A gold electrode modified with amino-modified reduced graphene oxide, ion specific DNA and DNAzyme for dual electrochemical determination of Pb(II) and Hg(II), Microchim. Acta 182 (2015) 2251–2258.
[40] M. Ebrahimi. J.B. Raoof, R. Ojani, Novel electrochemical DNA hybridization biosensors for selective determination of silver ions, Talanta 144 (2016) 619–626.
[41] C. Tortolini, P. Bollella, M.L. Antonelli, R. Antiochia, F. Mazzei, G. Favero, DNA-based biosensors for Hg^{2+}determination by polythymine-methylene blue modified electrodes, Biosens. Bioelectron. 67 (2015) 524–531.
[42] M. Jarczewska, Ł. Górski, E. Malinowska, Application of DNA aptamers as sensing layers for electrochemical detection of potassium ions, Sens. Actuators, B 226 (2016) 37–43.
[43] M. Jarczewska, E. Kierzkowska, R. Ziółkowski, Ł. Górski, E. Malinowska, Electrochemical oligonucleotide-based biosensor for the determination of lead ion, Bioelectrochem. 101 (2015) 35–41.
[44] A. Bala, Ł. Górski, Determination of mercury cation using electrode modified with phosphorothioate oligonucleotide, Sens. Actuators, B 230 (2016) 731–735.
[45] A. Bala, M. Pietrzak, Ł. Górski, E. Malinowska, Electrochemical determination of lead ion with DNA oligonucleotide-based biosensor using anionic redox marker, Electrochim. Acta 180 (2015) 763–769.
[46] E.L.S. Wong, J.J. Gooding, Charge transfer through DNA: A selective electrochemical DNA biosensor, Anal. Chem. 78 (2006) 2138–2144.

Figure Captions

Scheme 1. Schematic representation of the PNA-based biosensor response towards Hg^{2+} (M) with AQMS-Na (–) as a redox marker. Mixture of single strands of PNA and MCH are immobilized at the surface of gold electrode.

Figure 1. The effect of various redox markers on electrode response. All measurement were conducted in 10 mmol·L^{-1} Tris, pH 6.0, containing 1 mmol·L^{-1} AQMS-Na/1 mmol·L^{-1} $K_3[Fe(CN)_6]/K_4[Fe(CN)_6]$ (1:1) in 0.1 mol·L^{-1} KCl/10 µmol·L^{-1} RuHex/10 µmol·L^{-1} MB before and after addition of Hg^{2+} with final concentration of 10 µmol·L^{-1}. Error bar represents the standard deviation of six repetitive experiments.

Figure 2. Square wave voltammograms of 10 mmol·L^{-1} Tris, pH 6.0, containing A) 1 mmol·L^{-1} AQMS-Na and B) 1 mmol·L^{-1} $K_3[Fe(CN)_6]/K_4[Fe(CN)_6]$ (1:1) in 0.1 mol·L^{-1} KCl. Measurements for: (I) bare gold electrode; (II) gold electrode modified with PNA probe before and (III) after incubation in 10 µmol·L^{-1} $HgCl_2$.

Figure 3. A) Influence of backbone modification (PNA or DNA) on the electrochemical response of electrodes in the presence of AQMS-Na or $Fe^{II/III}$ used as a redox marker. All measurement were conducted in 10 mmol·L^{-1} Tris, pH 6.0, containing 1 mmol·L^{-1} AQMS-Na or 1 mmol·L^{-1} $K_3[Fe(CN)_6]/K_4[Fe(CN)_6]$ (1:1) in 0.1 mol·L^{-1} KCl before and after addition of Hg^{2+} with final concentration 10 µmol·L^{-1}. Error bar represents the standard deviation of six repetitive experiments. B) Plots of redox peak currents *vs* the square root of scan rate (from 5 to 500 mV·s^{-1}) before (curve I) and after (curve II) incubation in Hg^{2+}. Experiments were performed in 10 mmol·L^{-1} Tris, pH 6.0, containing 1 mmol·L^{-1} AQMS-Na.

Figure 4. Nyquist plots of a gold disc electrode. (I) Bare gold electrode; (II) electrode with PNA receptor layer; (III) analysis after 60 min incubation in 10 µmol·L^{-1} Hg^{2+}. All measurements were conducted in 10 mmol·L^{-1} Tris solution containing 1 mmol·L^{-1} AQMS-Na (pH 6.0). Z′ is the real impedance component and −Z″ is the imaginary impedance component. Inset: Randles equivalent circuit for proposed biosensor.

Figure 5. Calibration curve for PNA-modified gold electrode towards Hg^{2+} (sample incubation time of 60 min). Inset: calibration curve as a dependence between current changes and logarithm of Hg^{2+} concentration in the range from $5{\cdot}10^{-9}$ to $5{\cdot}10^{-7}$ mol·L^{-1}. The calibration equation is y = 0,4060x + 3,4785 with a correlation coefficient of 0.9900, where x refers to logarithm of mercury ion concentration ($\log[Hg^{2+}]/mol{\cdot}L^{-1}$) and y to $((I - I_0)/I_0)$; error bars show the standard deviations of measurements from six independent experiments.

Figure 6. Selectivity of electrodes modified with PNA sequence. (A) All cations were at 10 µmol·L^{-1} concentration. "Mix" was a sample containing all tested ions at 10 µmol·L^{-1} concentration. The measurements were performed in 10 mmol·L^{-1} Tris solution containing 1 mmol·L^{-1} AQMS-Na (pH 6.0). (B) Electrode response for lower concentration of Hg^{2+}, K^+ and mixture of Hg^{2+} and K^+. Error bar represents the standard deviation of six repetitive experiments.

Scheme 1

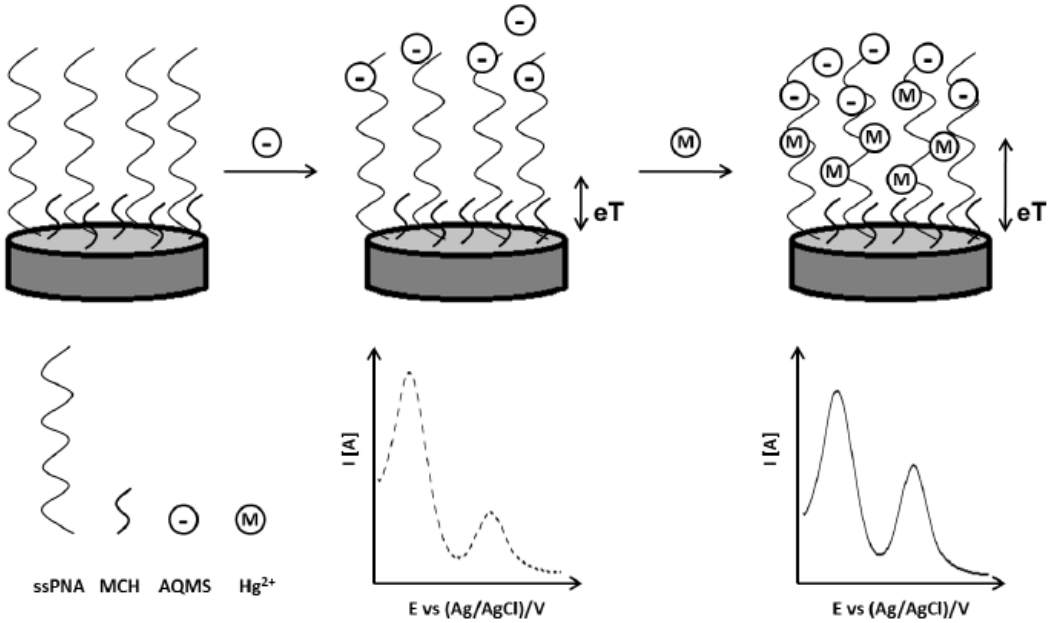

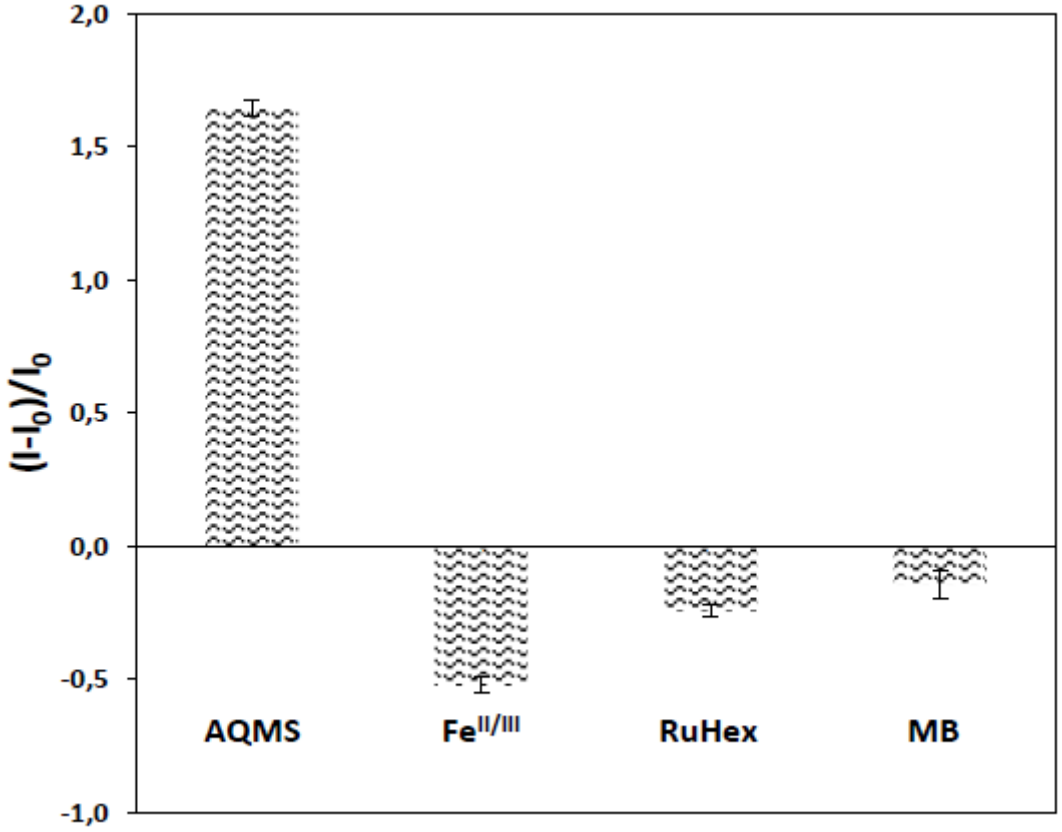

Figure 1

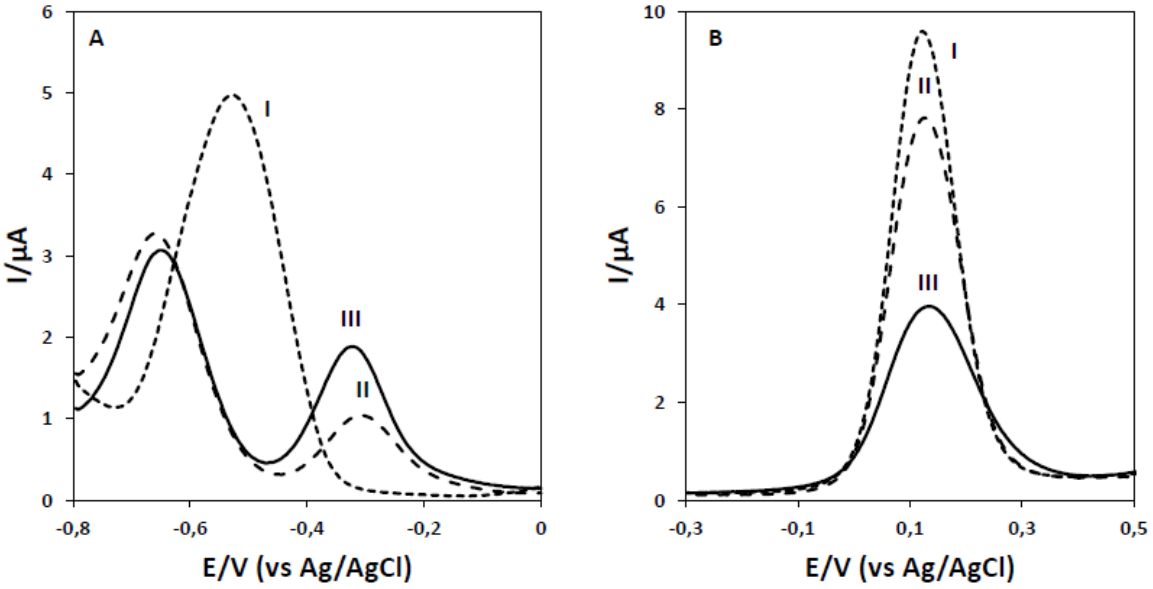

Figure 2

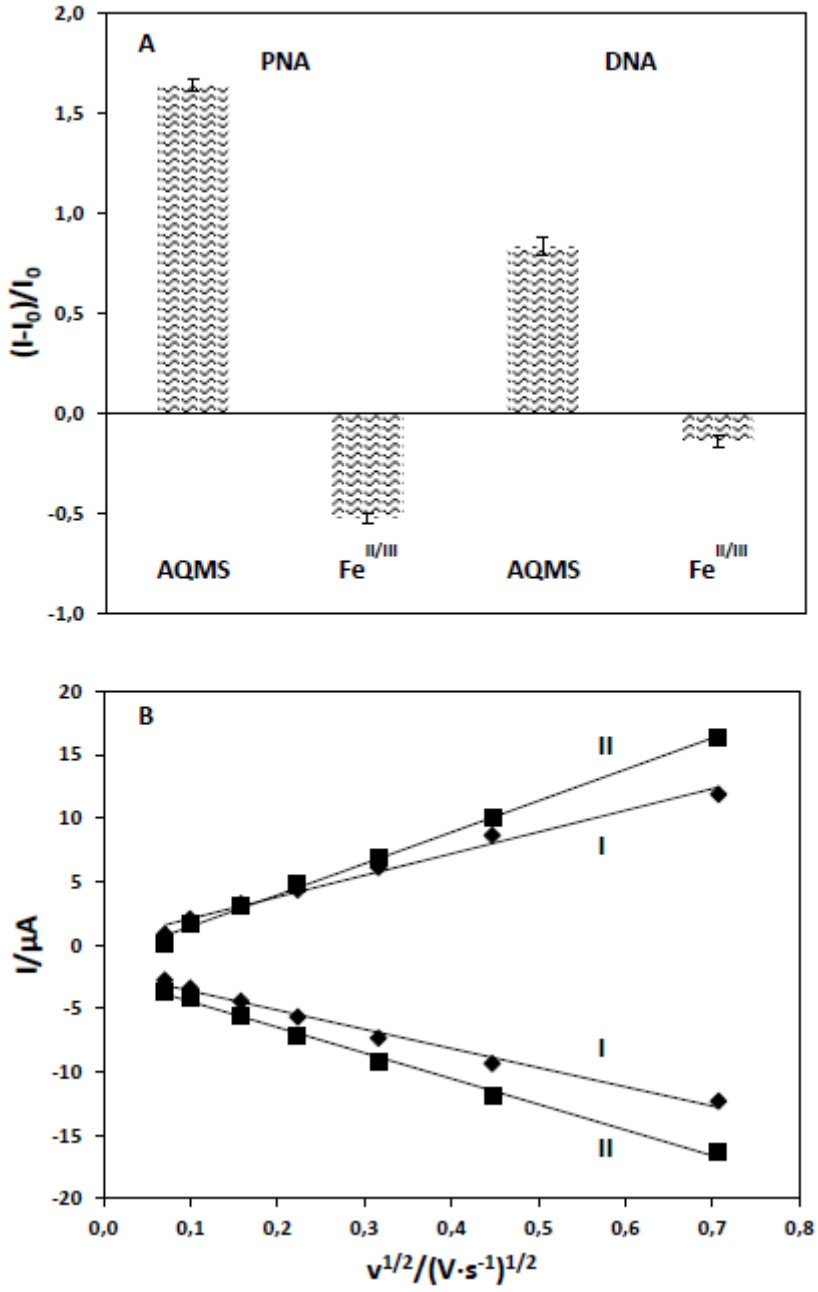

Figure 3

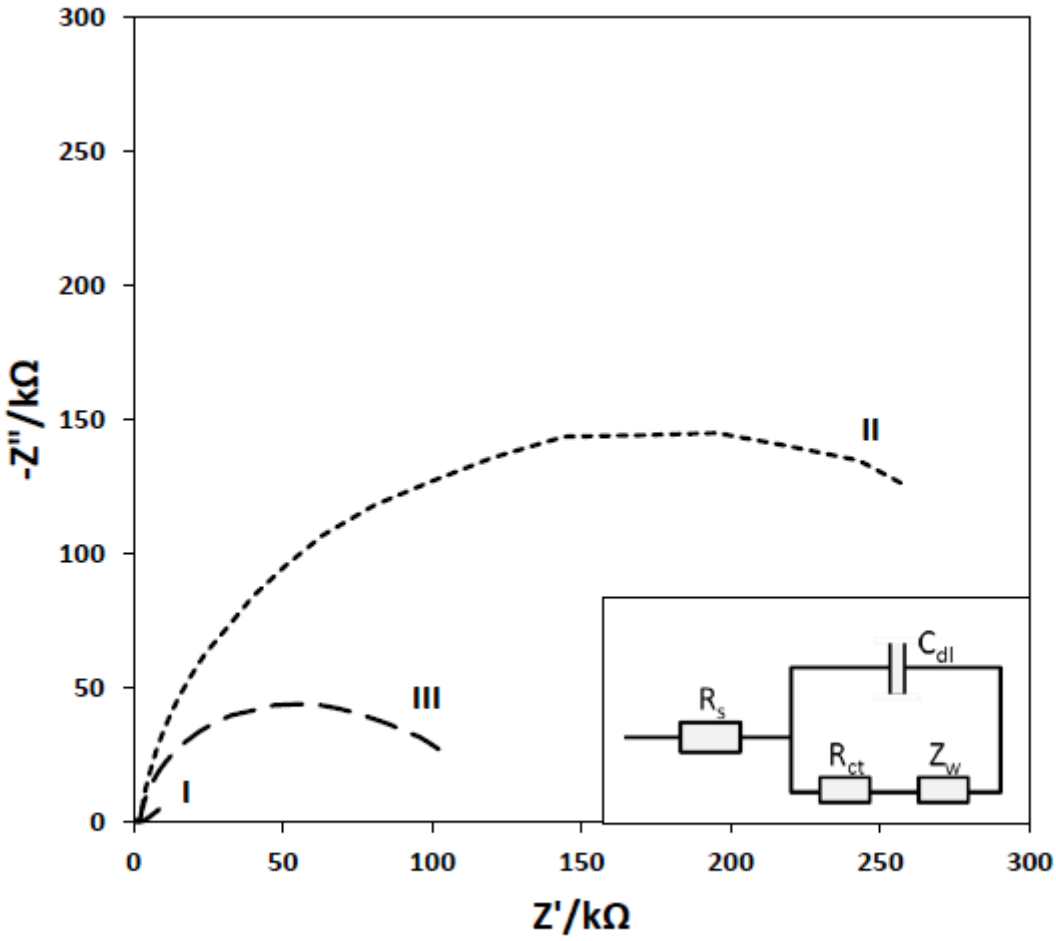

Figure 4

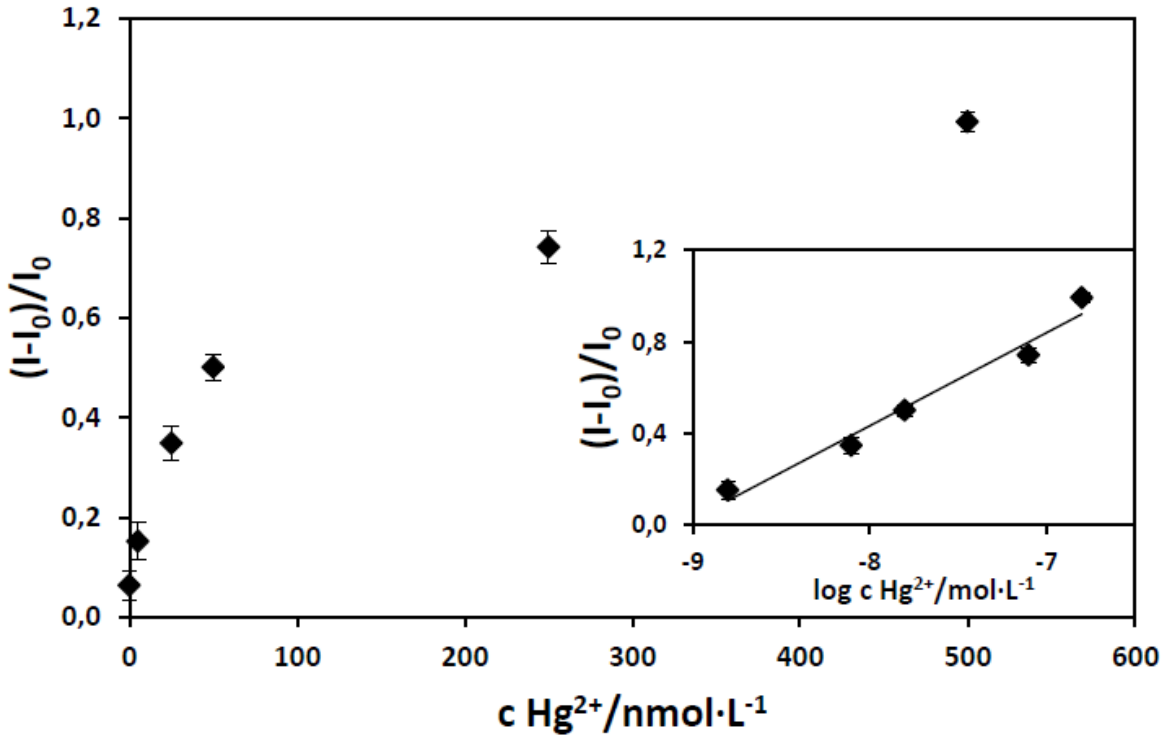

Figure 5

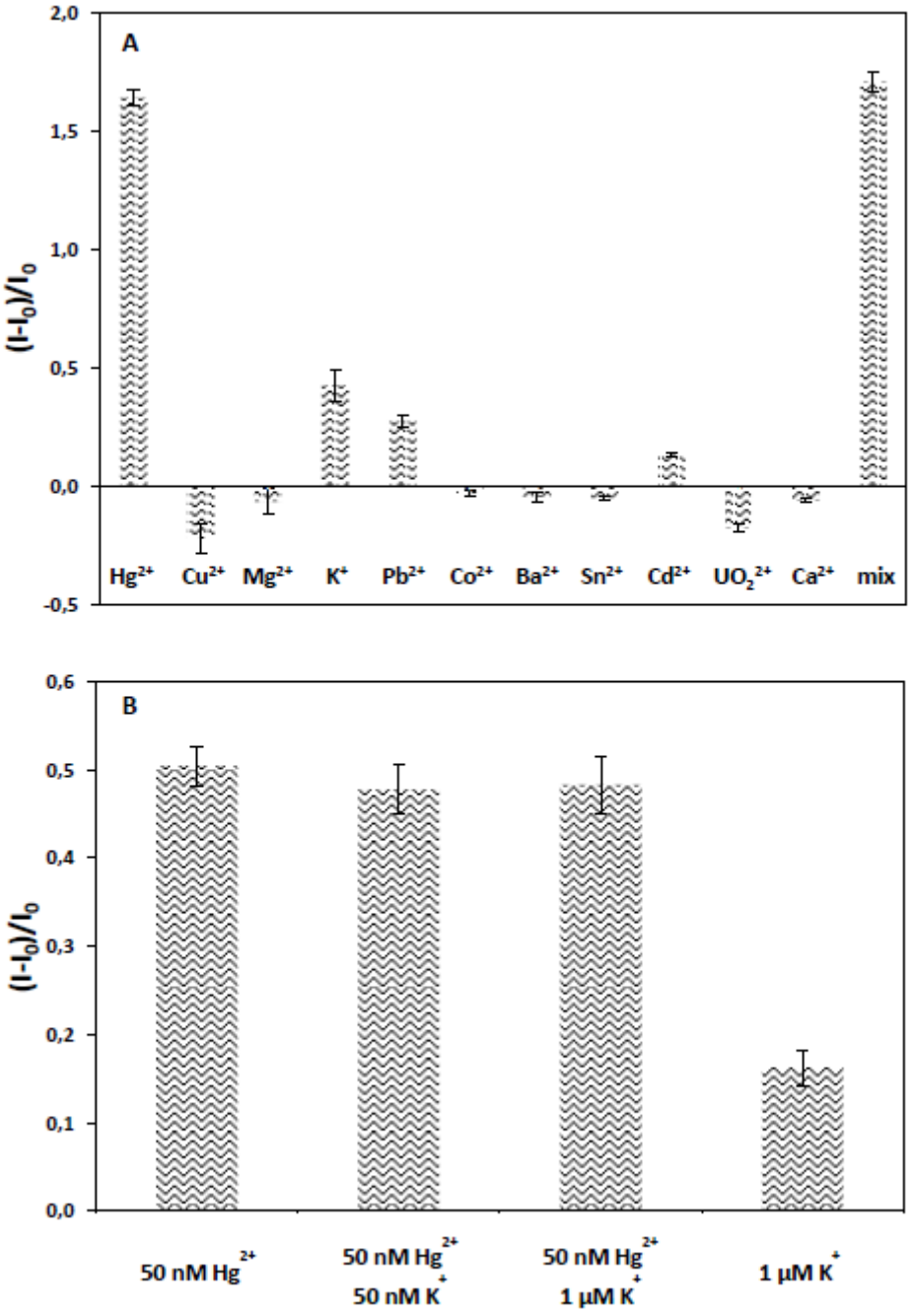

Figure 6

Highlights

- PNA-modified electrodes for the determination of mercury cation were developed.
- PNA was immobilized via –SH group on gold dics electrode.
- AQMS was used as a redox marker for the generation of current signal.
- High selectivity towards mercury cation and lower detection limit of 4.45 nmol·L^{-1} were observed.